ORGANOMETALLICS

Article

pubs.acs.org/Organometallics

Configurational Isomerization of Dinuclear Iridium and Rhodium Complexes with a Series of NPPN Ligands, 2-PyCH$_2$(Ph)P(CH$_2$)$_n$P(Ph)CH$_2$-2-Py (Py = Pyridyl, n = 2−4)

Takayuki Nakajima,* Yuki Fukushima, Minori Tsuji, Naoko Hamada, Bunsho Kure, and Tomoaki Tanase*

Department of Chemistry, Faculty of Science, Nara Women's University, Kitauoya-nishi-machi, Nara 630-8506, Japan

Supporting Information

ABSTRACT: New heterodonor NPPN tetradentate ligands, 2-PyCH$_2$(Ph)P(CH$_2$)$_n$P(Ph)CH$_2$-2-Py (*meso*- and *rac*-L^n; n = 2−4, Py = pyridyl), were prepared and reacted with [Cp*MCl$_2$]$_2$ (M = Ir, Rh; Cp* is pentamethylcyclopentadienyl) in the presence of NH$_4$BF$_4$ to afford a series of dinuclear complexes [(Cp*MCl)$_2$(*meso*-L^n)](BF$_4$)$_2$ (M = Ir, n = 2 (**2a**), 3 (**3a**), 4 (**4a**); M = Rh, n = 2 (**2c**), 3 (**3c**), 4 (**4c**)) and [(Cp*MCl)$_2$(*rac*-L^n)](BF$_4$)$_2$ (M = Ir, n = 2 (**2b**), 3 (**3b**), 4 (**4b**); M = Rh, n = 2 (**2d**), 3 (**3d**), 4 (**4d**)), which were characterized by IR, ^{1}H and ^{31}P{^{1}H} NMR, and ESI mass spectroscopic techniques and X-ray crystallography. The configurations around the two metal centers were controlled by the configuration of the coordinated P atoms so as to avoid repulsive interaction between the phenyl group on P and the chloride ligand, resulting in the formation of stereospecific isomers; a *meso* configuration of the metal centers is induced from *meso*-L^n (abbreviated as *meso*-P$_2$/*meso*-M$_2$), and in contrast, a *rac* configuration is induced from *rac*-L^n (*rac*-P$_2$/*rac*-M$_2$). Furthermore, inversion of metal centers for the Ir$_2$ complexes occurred in DMSO at higher temperatures (60−100 °C), generating equilibrium mixtures of minor diastereomers (*meso*-P$_2$/*rac*-M$_2$ or *rac*-P$_2$/*meso*-M$_2$) in low ratios together with the major isomers (*meso*-P$_2$/*meso*-M$_2$ or *rac*-P$_2$/*rac*-M$_2$). The equilibrium constants, K = [minor isomer]/[major isomer], varied appreciably depending on the lengths of the methylene chains as well as configurations of the NPPN ligands; the overall propensity for the K values was observed to be L^2 < L^3 < L^4 and *meso*-L^n < *rac*-L^n, while *rac*-L^3, *rac*-L^4, and *meso*-L^4 showed almost identical equilibrium constants, presumably resulting from no steric influence between the two metal centers.

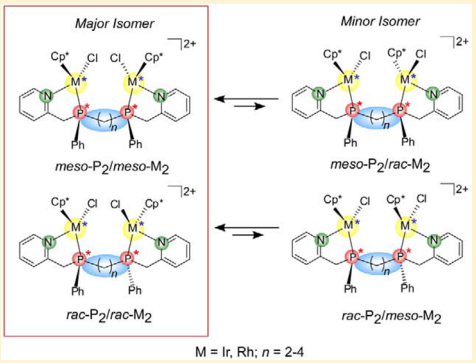

INTRODUCTION

The design of multidentate ligands is of crucial importance to fabricate functional metal centers and thus remains a main subject in modern molecular sciences of inorganic and organometallic chemistry with relevance to a wide variety of valuable applications.[1] In particular, multidentate mixed-donor ligands have attracted considerable recent interest because they should notably involve (1) hemilabile chelating effects that stabilize and activate the metal center and (2) bridging effects that connect two or more metals and induce cooperative and synergistic functions exerted by the metals.[2,3] There have been a number of studies on mononuclear transition-metal complexes with PN heterodonor ligands, which are attractive as homogeneous catalysts because the hard−soft and hemilabile characters of PN ligands permit metal coordination sites suitable for substrate binding and activation.[4] Dinucleating ligands with PN heterodonor units are usually concerned with PNNP tetradentate systems, in which diphenylphosphino and diphenylphosphinomethyl groups are incorporated into rigid N-donor scaffolds such as 2,2′-bipyridyl, 1,10-phenanthroline, 1,8-naphthylidine, pyrazole, phthalazine, and so on.[5] In contrast, examples are quite limited with NPPN ligands, in which terminal N-donor units such as pyridyl and quinolinemethyl groups are connected to flexible diphosphine chains,[6] owing to the difficulty of separating stereoisomers arising from chirality of the P atoms, while unique reactivity may be induced by cooperation of two flexibly linked, adjacent hemilabile metal centers.

In the present study, we have prepared the new series of NPPN tetradentate ligands 2-PyCH$_2$(Ph)P(CH$_2$)$_n$P(Ph)CH$_2$-2-Py (L^n; n = 2−4, Py = pyridyl), where two phosphorus atoms with 2-picolyl substituent groups are connected with methylene chains of variable length with the aim of tuning the separation of two metal centers. With respect to the chirality of the P atoms, the NPPN ligands exist as *meso* and *racemic* diastereomers and both are able to capture two Cp*MCl (M = Ir^{III}, Rh^{III}) fragments to afford the series of dinuclear complexes [(Cp*MCl)$_2$(*meso*-L^n)](BF$_4$)$_2$ (M = Ir, n = 2 (**2a**), 3 (**3a**), 4 (**4a**); M = Rh, n = 2 (**2c**), 3 (**3c**), 4 (**4c**)) and [(Cp*MCl)$_2$(*rac*-L^n)](BF$_4$)$_2$ (M = Ir, n = 2 (**2b**), 3 (**3b**), 4 (**4b**); M = Rh, n = 2 (**2d**), 3 (**3d**), 4 (**4d**)). X-ray analyses of

Received: October 2, 2013
Published: November 22, 2013

the solid-state structures indicated that the configuration of the two metal centers was regulated by the configuration of the coordinated P atoms to form stereospecific isomers, in which a *meso* configuration for the metal centers is derived from *meso*-L^n and, in contrast, a *rac* configuration of the metal centers is derived from *rac*-L^n. In addition, inversion of metal centers for the Ir_2 complexes was found to occur in DMSO at higher temperatures (60−100 °C), affording equilibrium mixtures of the major and minor isomers with the equilibrium constants appreciably varying depending on the lengths of the methylene chains as well as the configuration of the NPPN ligands.

RESULTS AND DISCUSSION

Synthesis of NPPN Tetradentate Ligands *meso/rac*-L^n (n = 2−4). A new series of NPPN tetradentate ligands *meso-/rac*-L^n (n = 2−4) were synthesized as shown in Scheme 1.

Scheme 1. Preparations of NPPN Tetradentate Ligands, *meso*- and *rac*-L^n (n = 2−4)

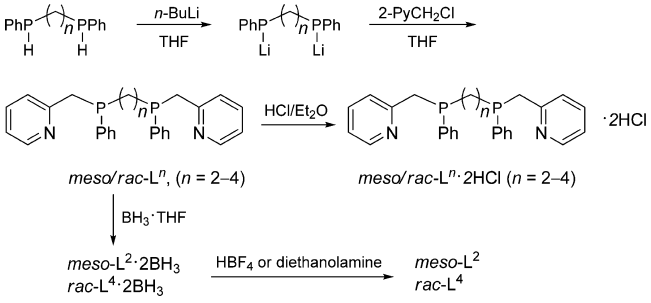

Deprotonation of $Ph(H)P(CH_2)_nP(H)Ph$ with *n*-BuLi and subsequent addition of picolyl chloride afforded 1:1 mixtures of *meso* and *rac* isomers of the NPPN ligands L^n in moderate yields which were monitored by $^{31}P\{^1H\}$ NMR spectroscopy (δ −14.8, −15.4 (L^2); δ −19.6, −19.7 (L^3); δ −18.5, −19.7 (L^4)) in $CDCl_3$. Addition of HCl dissolved in Et_2O to a solution of *meso-/rac*-L^n in Et_2O yielded the HCl adducts *meso-/rac*-L^n·2HCl as white solids, which were used for the synthesis of complexes without further purification.

While attempts to separate the stereoisomers of *meso-/rac*-L^n and *meso-/rac*-L^n·2HCl by crystallization were generally unsuccessful, *meso*-L^2 and *rac*-L^4 ligands were able to be isolated on a millimole scale successfully via their phosphine−borane adducts. Treatment of *meso-/rac*-L^2 and *meso-/rac*-L^4 with BH_3−THF, followed by precipitation from MeOH, afforded white crystals of *meso*-L^2·$2BH_3$ and *rac*-L^4·$2BH_3$ in 12 and 18% yields, respectively. The solid-state structures of *meso*-L^2·$2BH_3$ and *rac*-L^4·$2BH_3$ were determined by X-ray crystallography as shown in Figures S1 and S2 (see the Supporting Information). The removal of BH_3 from *meso*-L^2·$2BH_3$ and *rac*-L^4·$2BH_3$ was accomplished by treatment with diethanolamine or tetrafluoroboric acid to afford the desired *meso*-L^2 and *rac*-L^4 ligands in almost quantitative yields.

Synthesis of Dinuclear Iridium and Rhodium Complexes [(Cp*MCl)$_2$(*meso*-L^n)](BF$_4$)$_2$ and [(Cp*MCl)$_2$(*rac*-L^n)](BF$_4$)$_2$ (M = Ir, Rh, n = 2−4). Reactions of $[Cp^*MCl_2]_2$ (M = Ir (**1a**), Rh (**1b**)) with 1:1 *meso* and *rac* mixtures of the HCl adducts of NPPN ligands (*meso-/rac*-L^n·2HCl, n = 2−4) and excess NH_4BF_4 in the presence of NEt_3 in CH_2Cl_2 yielded the respective mixtures of $[(Cp^*MCl)_2(meso\text{-}L^n)](BF_4)_2$ and $[(Cp^*MCl)_2(rac\text{-}L^n)](BF_4)_2$ in a ca. 1:1 ratio (Scheme 2), which were separated by silica gel column chromatography

Scheme 2. Preparations of 2a−d, 3a−d, and 4a−d

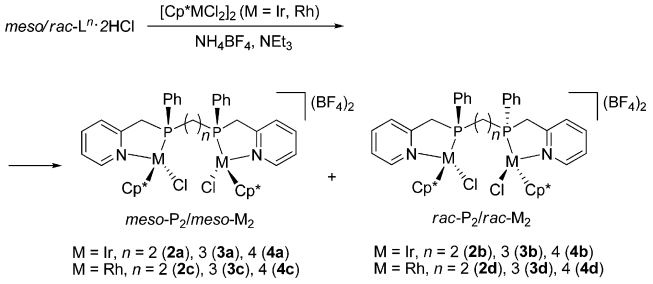

and/or crystallization, to isolate the series of dinuclear metal complexes $[(Cp^*MCl)_2(meso\text{-}L^n)](BF_4)_2$ (M = Ir, n = 2 (**2a**), 3 (**3a**), 4 (**4a**); M = Rh, n = 2 (**2c**), 3 (**3c**), 4 (**4c**)) and $[(Cp^*MCl)_2(rac\text{-}L^n)](BF_4)_2$ (M = Ir, n = 2 (**2b**), 3 (**3b**), 4 (**4b**); M = Rh, n = 2 (**2d**), 3 (**3d**), 4 (**4d**)), even though the isolated yields were extremely low. By using the pure isomers of *meso*-L^2 and *rac*-L^4, complexes **2a,c** and **4b,d** were obtained in good yields. While the six configurational isomers are potentially generated from the chirality of the two phosphorus atoms and the two metal centers (Scheme 3), the $^{31}P\{^1H\}$

Scheme 3. Stereoisomers of [(Cp*MCl)$_2$(*meso*- or *rac*-L^n)]$^{2+}$ (M = Ir, Rh; n = 2−4)

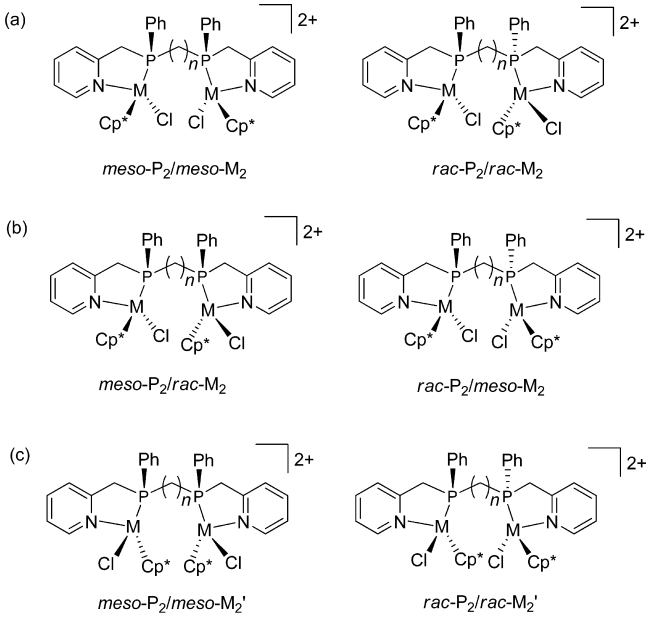

NMR spectra of the isolated complexes showed only one singlet corresponding to the major isomers, *meso*-P_2/*meso*-M_2 and *rac*-P_2/*rac*-M_2 (Scheme 3a), which were unambiguously determined by X-ray crystallography (Figure 1). The ORTEP diagrams for the complex cations of **2a,b**, **3a**, **3d′**, and **4a,b** are illustrated in Figure 1, and those of **2c** and **4d** are supplied in the Supporting Information (Figures S3 and S4). The crystallographic data and selected structural parameters are given in Tables S2−S4 in the Supporting Information. In all of the structures, two Cp*MCl fragments were chelated by 2-$PyCH_2P$ moieties to form a three-legged piano-stool structure and bridged by the central $P(CH_2)_nP$ diphosphine chains without any metal−metal interactions. The Cp*MCl(2-$pyCH_2(Ph)P$) structures are almost identical irrespective of the metal species, Ir or Rh, and the length of the diphosphine

dx.doi.org/10.1021/om400965j | Organometallics 2013, 32, 7470−7477

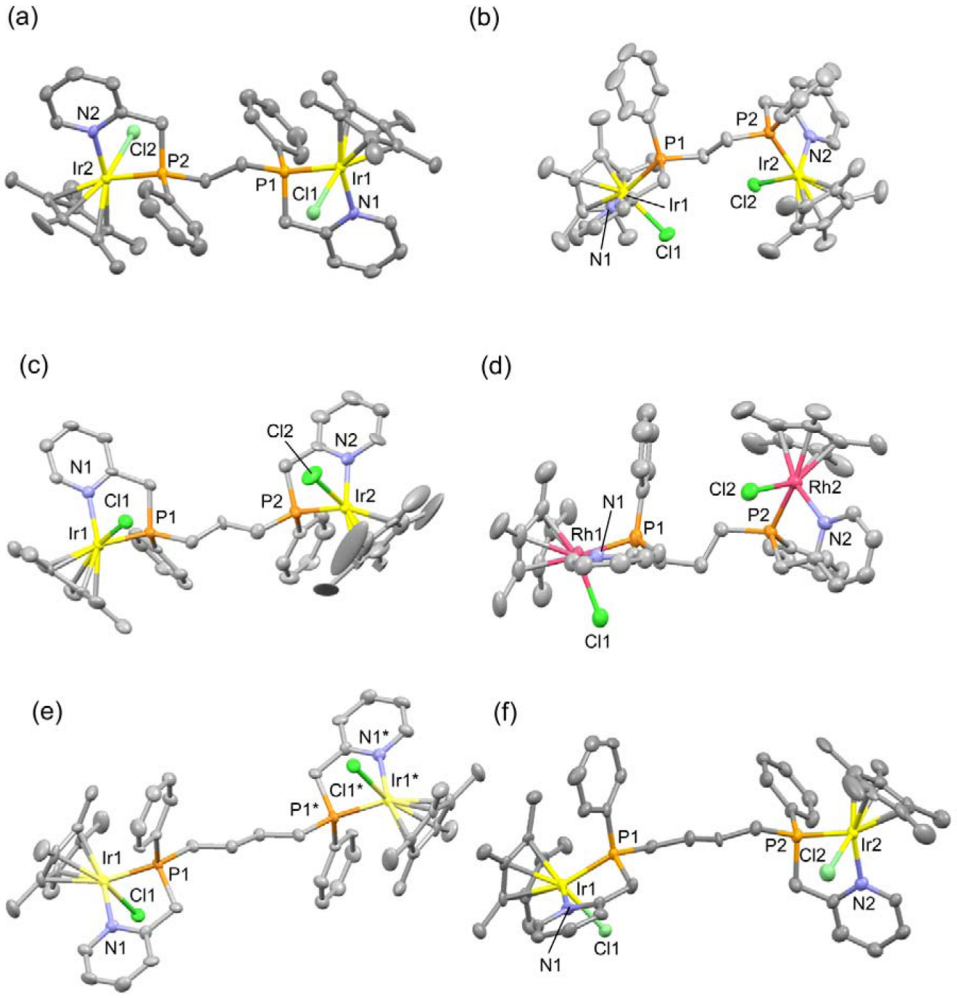

Figure 1. ORTEP diagrams for the complex cations of (a) **2a**, (b) **2b**, (c) **3a**, (d) **3d′**, (e) **4a**, and (f) **4b** with the atomic numbering schemes. The thermal ellipsoids are drawn at the 40% probability level, and the hydrogen atoms are omitted for clarity.

chains on the basis of the structural parameters given in Table S4 (Supporting Information): M−Cl = 2.386−2.414 Å, M−P = 2.260−2.295 Å, M−N = 2.093−2.154 Å, and P−M−Cl = 85.32−93.65°. The structures of **2a** (M = Ir) and **2c** (M = Rh) with *meso*-L^2 have pseudo or crystallographic C_i symmetry to reduce the steric repulsion between the two metal fragments of {Cp*MCl(2-pyCH$_2$(Ph)P)}, resulting in the metal−metal separations of 8.336(5) Å (**2a**) and 8.370(4) (**2c**) Å (Figure 1a and Figure S3 (Supporting Information)). On the other hand, the complex cation of **2b** (M = Ir) with *rac*-L^2 has a pseudo C_2 axis passing through the middle of the diphosphine chain (Figure 1b), where the metal−metal distance of 6.989(3) Å is remarkably shorter than those with *meso*-L^2. For the propylene-bridged complexes **3a** (M = Ir) and **3d′** (M = Rh), the former (**3a**) with *meso*-L^3 has a pseudo C_s symmetry (Figure 1c). However, the latter (**3d′**) with *rac*-L^3 possesses a pseudo C_2 symmetry as observed in **2b** (Figure 1d); the metal−metal separation of **3d′** (8.461(3) Å) is shorter by ca. 1.1 Å than that of **3a** (9.550(4) Å). For the butylene-bridged complexes, the structure of **4a** (M = Ir, Figure 1e) with *meso*-L^4 has an inversion center like that of **2c** and those of **4b** (M = Ir, Figure 1f) and **4d** (M = Rh, Figure S4 (Supporting Information)) with *rac*-L^4 adopting a pseudo C_2 symmetry as found in **2b** and **3d**. The metal−metal separation of 10.878(5) Å (**4a**) is slightly longer than those of **4b** (10.612(2) Å) and **4d** (10.613(3) Å). The distances between the two metal centers (d_{MM}) vary depending on the length (n) of the central methylene chains of the NPPN ligands (L^n) with the apparent propensity of d_{MM}(*meso*-L^n) > d_{MM}(*rac*-L^n) for the same number of n and $\Delta d_{MM}(L^2) > \Delta d_{MM}(L^3) > \Delta d_{MM}(L^4)$ for $\Delta d_{MM} = d_{MM}$(*meso*-L^n) − d_{MM}(*rac*-L^n), as shown in Figure S5 (Supporting Information).

The X-ray crystal structures clearly revealed that the configuration around the metal centers is completely regulated by the configuration of the coordinated P atoms so as to avoid steric repulsion between the phenyl group and the chloride ligand, resulting in the formation of stereospecific isomers in which the *meso* configuration for the metal centers is derived from *meso*-L^n (abbreviated as *meso*-P$_2$/*meso*-M$_2$) in **2a**,**c**, **3a**, and **4a**, and in contrast, a *rac* configuration of the metal centers is induced from *rac*-L^n (*rac*-P$_2$/*rac*-M$_2$) in **2b**, **3d′**, and **4b**,**d**. Because no influence depending on the length of diphosphine chains was observed, the preferential formations of the *meso*-P$_2$/*meso*-M$_2$ and *rac*-P$_2$/*rac*-M$_2$ isomers are attributed to steric repulsion between the chloride ligand attached to the metal ion and the phenyl substituent on the phosphorus atom (Figure 2). Since the preferred configuration of the {Cp*MCl(2-pyCH$_2$(Ph)P)} fragment is represented as R_M,R_P or S_M,S_P in CIP notation, the absolute configurations for the two M and two P centers are described as R_M,R_P,S_P,S_M for the stereoisomer

dx.doi.org/10.1021/om400965j | *Organometallics* 2013, 32, 7470−7477

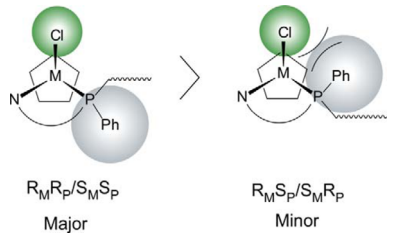

Figure 2. Repulsive interaction between the phenyl group of the P atom and the Cl ligand. R_M or S_M indicates the absolute configuration around the metal center and R_P or S_P that of the P atom.

of *meso*-P_2/*meso*-M_2, and as $S_M,S_P,S_P,S_M/R_M,R_P,R_P,R_M$ for the stereoisomer of *rac*-P_2/*rac*-M_2. These configurational structures were retained even in the solution state at room temperature, which was confirmed by $^{31}P\{^1H\}$ NMR spectra showing a singlet peak at δ 17.9−20.5 ppm for the two equivalent phosphorus atoms of the iridium complexes (**2a,b, 3a,b, 4a,b**), and a doublet peak at δ 47.9−49.9 ppm with $^1J_{RhP}$ = 132−136 Hz for those of the rhodium complexes (**2c,d, 3c,d, 4c,d**). Furthermore, the $^{31}P\{^1H\}$ NMR spectra of the reaction mixtures of $[Cp^*MCl_2]_2$ with L^n·2HCl also indicated that the *meso*-P_2/*meso*-M_2 and *rac*-P_2/*rac*-M_2 isomers (Scheme 3a) were formed dominantly as major products together with only small amounts of the minor isomers, as shown in Scheme 3b,c.

Equilibrium Studies. Although the *meso*-M_2/*meso*-P_2 and *rac*-M_2/*rac*-P_2 structures were retained in the solution state at room temperature, inversion of the metal centers for the iridium complexes occurred in DMSO upon increasing temperature at 60−100 °C to afford equilibrium mixtures of the major (*meso*-P_2/*meso*-M_2 or *rac*-P_2/*rac*-M_2) and minor (*meso*-P_2/*rac*-M_2 or *rac*-P_2/*meso*-M_2) isomers, which were monitored by $^{31}P\{^1H\}$ NMR spectroscopy (Figure 3). The $^{31}P\{^1H\}$ NMR spectra of *meso*-P_2/*rac*-M_2 and *rac*-P_2/*meso*-M_2 isomers showed two resonances due to the presence of two nonequivalent phosphorus atoms. Inversion of metal centers seems to proceed through dissociation of chloride ligands.[13] The *meso*-P_2/*rac*-M_2 isomer ($R_M,R_P,S_P,R_M/S_M,R_P,S_P,S_M$) was formed from the *meso*-P_2/*meso*-M_2 isomer (for example **4a** in Figure 3a,b) and the *rac*-P_2/*meso*-M_2 isomer ($R_M,S_P,S_P,S_M/S_M,R_P,R_P,R_M$) from the *rac*-$P_2$/*rac*-$M_2$ isomer (for example **4b** in Figure 3c,d) via chiral inversion of one metal center. The doubly inverted isomers of *meso*-P_2/*meso*-M_2' (S_M,R_P,S_P,R_M) or *rac*-P_2/*rac*-M_2' ($R_M,S_P,S_P,R_M/S_M,R_P,R_P,S_M$) were estimated to be generated in very small amounts, which tentatively corresponded to the small singlet peaks marked with asterisks in Figure 3b,d. For the rhodium complexes **2c** and **4d**, heating of their DMSO solutions at higher temperature led to reaction mixtures containing a decomposed species and the isomers generated by configurational inversion of the metal centers, which prevented further detailed discussion.

The equilibrium constants of the two stereoisomers (K = [*meso*-P_2/*rac*-M_2]/[*meso*-P_2/*meso*-M_2] or [*rac*-P_2/*meso*-M_2]/[*rac*-P_2/*rac*-M_2]) of **2a,b**, **3a,b**, and **4a,b** were measured at various temperatures between 60 and 100 °C in DMSO-d_6 by integration of the $^{31}P\{^1H\}$ NMR resonances and indicated that the central methylene chains and the configurations of the NPPN ligands have appreciable influences on the isomerization (Figure 4). The K values apparently increase in the order *meso*-L^2 < *meso*-L^3 < *rac*-L^2 < *rac*-L^3 ≈ *meso*-L^4 ≈ *rac*-L^4. The overall propensity for the K values was observed to be $L^2 < L^3 < L^4$ and *meso*-L^n < *rac*-L^n, although *rac*-L^3, *rac*-L^4, and *meso*-L^4 showed almost identical equilibrium constants, presumably resulting from no steric influence existing between the two metal centers bridged by long methylene chains. In contrast, isomerization from **2a,b** and **3a** with *meso*-/*rac*-L^2 and *meso*-L^3 involve some steric influence between the two metal fragments, which should

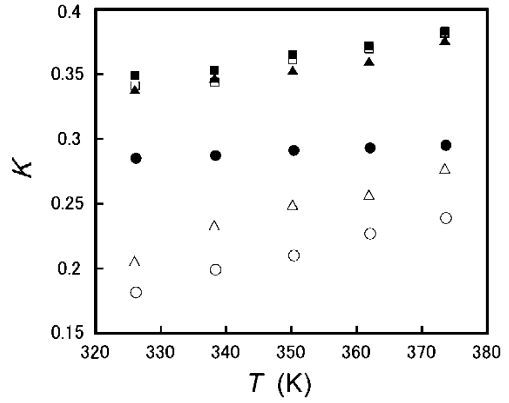

Figure 4. Plots of equilibrium constant K vs temperature in the reaction solutions from **2a** (○), **2b** (●), **3a** (△), **3b** (▲), **4a** (□), and **4b** (■).

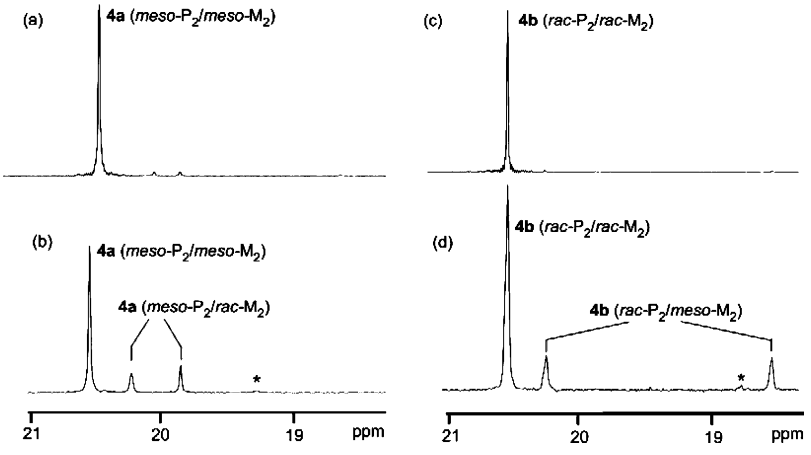

Figure 3. $^{31}P\{^1H\}$ NMR spectra in DMSO-d_6 of (a) **4a** at room temperature, (b) **4a** after heating at 100 °C, (c) **4b** at room temperature, and (d) **4b** after heating at 100 °C.

dx.doi.org/10.1021/om400965j | *Organometallics* 2013, 32, 7470−7477

Table 1. Thermodynamic Parameters of ΔH° and ΔS° Obtained from van't Hoff Plots for the Equilibrium Reactions from 2a–4a with *meso*-L^n (n = 2–4) and 2b–4b with *rac*-L^n (n = 2–4)[a]

	2a, *meso*-L^2	**2b**, *rac*-L^2	**3a**, *meso*-L^3	**3b**, *rac*-L^3	**4a**, *meso*-L^4	**4b**, *rac*-L^4
ΔH° (kJ/mol)	5.6(3)	0.79(5)	5.9(6)	2.1(3)	2.5(3)	2.0(2)
ΔS° (J/(K mol))	3.0(8)	−8(2)	5.2(18)	−2.5(8)	−1.3(8)	−2.7(5)

[a]See Figure S6 in the Supporting Information.

result in suppression of inversion around the metal centers. The van't Hoff plots of −ln K vs $1/T$ provided thermodynamic parameters of ΔH° and ΔS° (Table 1 and Figure S6). While the absolute values of ΔS° are very small in all, ΔH° values for the reactions from **2a** (*meso*-L^2) and **3a** (*meso*-L^3) are remarkably large in comparison with those for other complexes, suggesting that steric interaction between the two metal fragments prohibits the configurational inversion to some extent.

CONCLUSION

The series of dinuclear iridium and rhodium complexes $[(Cp^*MCl)_2(meso\text{-}L^n)]^{2+}$ and $[(Cp^*MCl)_2(rac\text{-}L^n)]^{2+}$ (M = Ir, Rh; n = 2–4) were synthesized by the reaction of new tetradentate NPPN ligands *meso*-/*rac*-L^n with $[Cp^*MCl_2]_2$. X-ray analyses of their solid-state structures revealed that the configurations of the two metal centers were determined by the configuration of the coordinated P atoms, resulting in the stereospecific formation of *meso*-P_2/*meso*-M_2 and *rac*-P_2/*rac*-M_2 isomers, avoiding steric repulsion between the chloride ligand and the phenyl substituent on the phosphorus atom. Configurational inversion of the metal centers for the iridium dinuclear complexes was investigated at higher temperatures, which demonstrated that the central methylene chains and the configurations of the NPPN ligands have considerable influence on the isomerization.

EXPERIMENTAL SECTION

General Considerations. All reactions were carried out under a nitrogen atmosphere by using standard Schlenk techniques. Solvents were dried by standard procedures and freshly distilled prior to use. Other reagents were used as purchased without further purification. The compounds $Ph(H)P(CH_2)_nP(H)Ph$ (n = 2–4) were prepared by the reported procedure.[7] ^1H and $^{31}P\{^1H\}$ NMR spectra were recorded on a JEOL JMN-AL-400 spectrometer at 400 and 160 MHz, respectively. The chemical shifts were calibrated to TMS (^1H) or 80% H_3PO_4 (^{31}P) as an external reference. IR spectra were measured on KBr pellets with a JASCO FT/IR-410 spectrometer. ESI-TOF-MS spectra were obtained with a JEOL JMS-T100LC high-resolution mass spectrometer with positive ionization mode.

General Procedure for Synthesis of *meso*- and *rac*-NPPN (*meso*/*rac*-L^n: n = 2–4) Ligands. To a solution of the diphenylphosphine $Ph(H)P(CH_2)_nP(H)Ph$ (n = 2–4) in THF was added dropwise 2 equiv of *n*-BuLi (1.57 M in hexane) at −78 °C. Then, 2 equiv of 2-picolyl chloride in THF was added at the same temperature. The cooling bath was removed, and the mixture was stirred overnight at room temperature before degassed H_2O was added. The organic phase was separated, and the aqueous phase was extracted with Et_2O. The combined organic extract was dried over Na_2SO_4, filtered, and concentrated under reduced pressure to a give mixture of *meso*- and *rac*-L^n ligands (n = 2–4).

meso- and rac-Bis{phenyl(2-picolyl)phosphine}ethane (meso/rac-L²). A mixture of *meso*- and *rac*-L^2 was obtained in 58% yield (5.21 g, 21.2 mmol) from 1,2-bis(diphenylphosphino)ethane. ^1H NMR ($CDCl_3$): δ 1.51–1.89 (m, 4H, CH_2CH_2), 3.15, 3.16 (s, 4H, $PyCH_2$), 6.76–7.35 (m, 16H, Ph, Py), 8.37 (br s, 2H, Py). $^{31}P\{^1H\}$ NMR ($CDCl_3$): δ −15.4 (s, 1P, *rac*), −14.8 (s, 1P, *meso*).

meso- and rac-Bis{phenyl(2-picolyl)phosphine}propane (meso/rac-L³). A mixture of *meso*- and *rac*-L^3 was obtained in 81% yield (2.37 g, 9.09 mmol) from 1,2-bis(diphenylphosphino)propane. ^1H NMR ($CDCl_3$): δ 1.21–1.63 (m, 4H, CH_2), 3.18–3.19 (m, 4H, $PyCH_2$), 6.76–8.40 (m, 18H, Ph, Py). $^{31}P\{^1H\}$ NMR ($CDCl_3$): δ −19.6 (s, 1P), −19.7 (s, 1P).

meso- and rac-Bis{phenyl(2-picolyl)phosphine}butane (meso/rac-L⁴). A mixture of *meso*- and *rac*-L^4 was obtained in 55% yield (1.43 g, 5.23 mmol) from 1,2-bis(diphenylphosphino)butane. ^1H NMR ($CDCl_3$): δ 1.24–2.46 (m, 8H, CH_2), 3.17–3.18 (m, 4H, $PyCH_2$), 6.80–8.42 (m, 26H, Ph, Py). $^{31}P\{^1H\}$ NMR ($CDCl_3$): δ −18.5 (s, 1P, *rac*), −19.7 (s, 1P, *meso*).

General Procedure for Synthesis of *meso*- and *rac*-NPPN·2HCl (*meso*-/*rac*-L^n·2HCl: n = 2–4) Ligands. To a solution of *meso*- and *rac*-NPPN (*meso*/*rac*-L^n: n = 2–4) ligands in Et_2O was added 4 equiv of HCl (1.57 M in Et_2O). The resulting white precipitate was filtered, washed with Et_2O, and dried under reduced pressure to give the ligands *meso*- and *rac*-NPPN·2HCl (*meso*-/*rac*-L^n·2HCl: n = 2–4), which were used without further purification for the synthesis of complexes.

meso- and rac-1,2-Bis{phenyl(2-picolyl)phosphino}ethane·2HCl (meso-/rac-L².2HCl). A mixture of *meso*- and *rac*-L^2·2HCl was obtained in 69% yield (5.28 g, 12.3 mmol) from *meso*/*rac*-L^2. $^{31}P\{^1H\}$ NMR (CD_3OD): δ −9.1 (s, 1P), −9.8 (s, 1P).

meso- and rac-1,3-Bis{phenyl(2-picolyl)phosphino}propane·2HCl (meso-/rac-L³·2HCl). A mixture of *meso*- and *rac*-L^3·2HCl was obtained in 76% yield (3.24 g, 7.32 mmol) from *meso*/*rac*-L^3. $^{31}P\{^1H\}$ NMR (CD_3OD): δ −12.7 (s, 1P), −12.6 (s, 1P).

meso- and rac-1,4-Bis{phenyl(2-picolyl)phosphino}butane·2HCl (meso/rac-L⁴·2HCl). A mixture of *meso*- and *rac*-L^4·2HCl was obtained in 83% yield (1.31 g, 2.87 mmol) from *meso*/*rac*-L^4. $^{31}P\{^1H\}$ NMR (CD_3OD): δ −11.6 (s, 1P).

***meso*-1,2-Bis{phenyl(2-picolyl)phosphino}ethane·2BH_3 (*meso*-L^2·2BH_3).** To a solution of *meso*-/*rac*-L^2 (4.7 g, 11.0 mmol) in THF (40 mL) was added BH_3–THF (30 mL, 33.0 mmo) at 0 °C. The mixture was stirred overnight at room temperature, and then degassed H_2O (30 mL) was added. The organic phase was separated, and the aqueous phase was extracted with AcOEt. The combined organic extracts were dried over Na_2SO_4, filtered, and concentrated under reduced pressure to give an oil. By addition of dry MeOH, white precipitates were formed, which were filtered off, washed with hexane, and dried under vacuum to afford white powders of *meso*-L^2·2BH_3 (531 mg, 12%). ^1H NMR ($CDCl_3$): δ 0.25–1.25 (br, 6H, BH_3), 1.89–2.01 (m, 2H, CH_2), 2.30–2.36 (m, 2H, CH_2), 3.36(m, 4H, $PyCH_2$), 6.87 (d, 2H, J = 8 Hz, Py), 7.06 (dd, 2H, J = 9, 5 Hz, Py), 7.36–7.53 (m, 12H, Ph, Py), 8.33 (d, 2H, J = 4 Hz, Py). $^{31}P\{^1H\}$ NMR ($CDCl_3$): δ 20.4 (br s, 2P).

***rac*-1,4-Bis{phenyl(2-picolyl)phosphino}butane·2BH_3 (*rac*-L^4·2BH_3).** To a solution of *meso*-/*rac*-L^4 (23.3 g, 51.0 mmol) in THF (40 mL) was added BH_3–THF (152 mL, 152 mmol) at 0 °C. The mixture was stirred overnight at room temperature before degassed H_2O (30 mL) was added. The organic phase was separated, and the aqueous phase was extracted with AcOEt. The combined organic extracts were dried over Na_2SO_4, filtered, and concentrated under reduced pressure to give an oil. By addition of dry MeOH, white precipitates were formed, which were filtered off, washed with hexane, and dried under vacuum to afford white powders of *rac*-L^4·2BH_3 (4.5 g, 18%). ^1H NMR ($CDCl_3$): δ 0.23–1.20 (br, 6H, BH_3), 1.31–1.45 (m, 2H, CH_2), 1.49–1.54 (m, 2H, CH_2), 1.85–1.92 (m, 4H, CH_2), 3.37 (d, 4H, J = 11 Hz, $PyCH_2$), 6.96 (d, 2H, J = 8 Hz, Py), 7.11 (t, 2H, J = 6 Hz, Py), 7.33–7.57 (m, 12H, Ph, Py), 8.33 (d, 2H, J = 4 Hz, Py). $^{31}P\{^1H\}$ NMR ($CDCl_3$): δ 16.8 (br d, 2P, J = 59 Hz).

dx.doi.org/10.1021/om400965j | *Organometallics* 2013, 32, 7470–7477

***meso*-1,2-Bis{phenyl(2-picolyl)phosphino}ethane (*meso*-L^2).** To a solution of *meso*-L^2·2BH$_3$ (400 mg, 0.0878 mmol) was added diethanolamine in MeOH at room temperature, and the mixture was heated at 100 °C for 2 h. After addition of degassed H_2O (20 mL), the mixture was heated at 80 °C. At room temperature, white precipitates were collected by filtration, washed with hexane, and dried under reduced pressure to afford white solids of *meso*-L^2 (357 mg, 95%). ^{1}H NMR ($CDCl_3$): δ 1.69−1.85 (m, 4H, CH_2), 3.18 (s, 4H, $PyCH_2$), 6.80 (d, 2H, J = 8 Hz, Py), 6.99 (dd, 2H, J = 9, 5 Hz, Py), 7.25−7.53 (m, 12H, Ph, Py), 8.40 (d, 2H, J = 4 Hz, Py). ^{31}P{^{1}H} NMR ($CDCl_3$): δ −14.8 (s, 2P).

***rac*-1,4-Bis{phenyl(2-picolyl)phosphino}butane (*rac*-L^4).** To a solution of *rac*-L^4·2BH$_3$ (200 mg, 0.40 mmol) in CH_2Cl_2 (20 mL) was added HBF_4 (1.5 mL, 11 mmol, 52.9 wt % in Et_2O), and the mixture was stirred overnight at room temperature. After addition of 1 M NaOH (12 mL, 12 mmol), the organic phase was separated and the aqueous phase was extracted with CH_2Cl_2. The combined organic extracts were dried over Na_2SO_4, filtered, and concentrated under reduced pressure to give a colorless oil of *rac*-L^4 (164 mg, 90%). ^{1}H NMR ($CDCl_3$): δ 1.36−1.41 (m, 4H, CH_2), 1.63−1.72 (m, 4H, CH_2), 3.18 (s, 4H, $PyCH_2$), 6.85 (d, 2H, J = 8 Hz, Py), 7.00 (t, 2H, J = 6 Hz, Py), 7.21−7.58 (m, 12H, Ph, Py), 8.44 (d, 2H, J = 4 Hz, Py). ^{31}P{^{1}H} NMR ($CDCl_3$): δ −18.5 (s, 2P).

General Procedure for Synthesis of [(Cp*MCl)$_2$(*meso*-L^n)](BF$_4$)$_2$ and [(Cp*MCl)$_2$(*rac*-L^n)](BF$_4$)$_2$ (M = Ir, Rh). *Method A.* To a solution of *meso*-/*rac*-L^n·2HCl (n = 2−4) in MeOH was added 4 equiv of NEt_3 at room temperature, and the solvent was removed under reduced pressure. To the residue was added CH_2Cl_2 (10 mL), 2 equiv of $[Cp^*MCl_2]_2$, and 5 equiv of NH_4BF_4 successively, and the mixture was stirred overnight at room temperature. After addition of degassed H_2O, the organic phase was separated and the aqueous phase was extracted with CH_2Cl_2. The combined organic extracts were dried over Na_2SO_4, filtered, and dried under reduced pressure. The residue was chromatographed on silica gel (eluent CH_2Cl_2/ MeOH 99/1) to separate it into [(Cp*MCl)$_2$(*meso*-L^n)](BF$_4$)$_2$ and [(Cp*MCl)$_2$(*rac*-L^n)](BF$_4$)$_2$, which were further purified by crystallization from CH_2Cl_2/Et_2O.

*[(Cp*IrCl)$_2$(meso-L^2)](BF$_4$)$_2$* ***(2a)*** *(Method A).* **2a** was obtained in 11% yield from crystallization (CH_2Cl_2/Et_2O) of the reaction mixture without column chromatography.

2a *(Method B).* To a solution of $[Cp^*IrCl_2]_2$ (44.9 mg, 0.0664 mmol) in CH_2Cl_2 (10 mL) were added a solution of *meso*-L^2 (28.4 mg, 0.0664 mmol) in CH_2Cl_2 (10 mL) and NH_4BF_4 (24.4 mg, 0.233 mmol), and the mixture was stirred overnight at room temperature before filtration. The filtrate was concentrated to ca. 3 mL. After addition of Et_2O (1 mL), the solution was allowed to stand in refrigerator to afford yellow crystals of **2a**. Yield: 31 mg, 35%. Anal. Calcd for $C_{46}H_{56}B_2Cl_2F_8Ir_2N_2OP_2$: C, 41.67; H, 4.04; N, 2.44. Found: C, 41.61; H, 4.25; N, 2.11. IR (KBr): ν 1473 (m), 1437 (m), 1084 (s), 1056 (s), 1034 (s) cm^{-1}. ESI-MS (MeOH): m/z 1241.01 (z1, [[(Cp*IrCl)$_2$(*meso*-L^2)](BF$_4$)]$^+$ (1241.26)). ^{1}H NMR (DMSO-d_6): δ 1.33 (s, 30H, Cp*), 1.80−1.84 (m, 2H, CH_2), 2.60−2.62 (m, 1H, CH_2), 3.58−3.62 (m, 1H, CH_2), 4.33−4.41 (m, 4H, $PyCH_2$), 6.85 (d, 2H, J = 8 Hz, Py), 7.00 (t, 2H, J = 6 Hz, Py), 7.21−7.58 (m, 12H, Ph, Py), 8.44 (d, 2H, J = 4 Hz, Py). ^{31}P{^{1}H} NMR (DMSO-d_6): δ 20.0 (s, 2P).

*[(Cp*IrCl)$_2$(rac-L^2)](BF$_4$)$_2$·5CHCl$_3$* ***(2b·5CHCl$_3$)*** *(Method A).* Yield: 2%. IR (KBr): ν 1472 (m), 1437 (m), 1083 (s), 1056 (s), 1034 (s) cm^{-1}. ESI-MS (MeOH): m/z 1241.35 (z1, [[(Cp*IrCl)$_2$(*rac*-L^2)](BF$_4$)]$^+$ (1241.26)). ^{1}H NMR (DMSO-d_6): δ 1.33 (s, 30H, Cp*), 1.80−3.21 (m, 4H, CH_2), 4.32 (m, 4H, $PyCH_2$), 7.40−8.51 (m, 28 H, Ph, Py). ^{31}P{^{1}H} NMR (DMSO-d_6): δ 20.5 (s, 2P). The formula was determined by X-ray crystallography because only a small amount of the pure sample was isolated.

*[(Cp*RhCl)$_2$(meso-L^2)](BF$_4$)$_2$* ***(2c)*** *(Method A).* **2c** was obtained in 11% yield from crystallization (CH_2Cl_2/Et_2O) of the reaction mixture without column chromatography.

2c *(Method B).* To a solution of $[Cp^*RhCl_2]_2$ (43.5 mg, 0.0704 mmol) in CH_2Cl_2 (5 mL) were added a solution of *meso*-L^2 (30.3 mg, 0.0708 mmol) in CH_2Cl_2 (10 mL) and NH_4BF_4 (30.0 mg, 0.286 mmol), and the mixture was stirred overnight at room temperature before filtration. The filtrate was concentrated to ca. 3 mL. After addition of Et_2O (1 mL), the solution was allowed to stand in refrigerator to afford yellow crystals of **2c**. Yield: 20 mg, 25%. Anal. Calcd for $C_{46}H_{56}B_2Cl_2F_8N_2P_2Rh_2$: C, 48.08; H, 4.91; N, 2.44. Found: C, 48.05; H, 4.67; N, 2.73. IR (KBr): ν 1473 (m), 1435 (m), 1083 (s), 1062 (s) cm^{-1}. ESI-MS (MeOH): m/z 1060.97 (z1, [[(Cp*RhCl)$_2$(*meso*-L^2)](BF$_4$)]$^+$ (1061.14)). ^{1}H NMR (DMSO-d_6): δ 1.31 (d, 30H, J = 3 Hz, Cp*), 1.80−1.84 (m, 2H, CH_2), 2.61−2.66 (m, 2H, CH_2), 4.33 (d, 4H, J = 11 Hz, $PyCH_2$), 7.54−7.58 (m, 12H, Ph, Py), 7.83 (d, 2H, J = 8 Hz, Py), 8.12 (t, 2H, J = 8 Hz, Py), 8.53 (d, 2H, J = 6 Hz, Py). ^{31}P{^{1}H} NMR (DMSO-d_6): δ 49.7 (dt, 2P, J_{P-Rh} = 136 Hz, $J_{P-P'}$ = 25 Hz).

*[(Cp*RhCl)$_2$(rac-L^2)](BF$_4$)$_2$* ***(2d)*** *(Method A).* Yield: 10%. IR (KBr): ν 1472 (m), 1437 (m), 1084 (s), 1056 (s), 1034 (s) cm^{-1}. ESI-MS (MeOH): m/z 1061.17 (z1, [[(Cp*RhCl)$_2$(*rac*-L^2)](BF$_4$)]$^+$ (1061.14)). ^{31}P{^{1}H} NMR (DMSO-d_6): δ 48.5 (dt, 2P, J_{P-Rh} = 135 Hz, $J_{P-P'}$ = 25 Hz). Elemental analysis was not performed because only a small amount of the pure sample was isolated.

*[(Cp*IrCl)$_2$(meso-L^3)](BF$_4$)$_2$* ***(3a)*** *(Method A).* **3a** was obtained in 15% yield from crystallization (CH_2Cl_2/Et_2O) of the reaction mixture without column chromatography. Anal. Calcd for $C_{47.5}H_{59}B_2Cl_3F_8Ir_2N_2P_2$: C, 41.21; H, 4.30; N, 2.02. Found: C, 41.36; H, 4.04; N, 2.29. IR (KBr): ν 1472 (m), 1437 (m), 1082 (s), 1060 (s), 1036 (s) cm^{-1}. ESI-MS (MeOH): m/z 1255.36 (z1, [[(Cp*IrCl)$_2$(*meso*-L^3)](BF$_4$)]$^+$ (1255.27)). ^{1}H NMR (DMSO-d_6): δ 1.41 (s, 30H, Cp*), 1.74 (m, 2H, CH_2), 2.42 (m, 2H, CH_2), 2.81 (m, 2H, CH_2), 4.11−4.30 (m, 4H, $PyCH_2$), 7.49 (m, 6H, Ph, Py), 7.57 (br s, 6H, Ph), 7.80 (d, 2H, J = 8 Hz, Py), 8.08 (d, 2H, J = 8 Hz, Py), 8.62 (d, 2H, J = 6 Hz, Py). ^{31}P{^{1}H} NMR (DMSO-d_6): δ 17.9 (s, 2P).

*[(Cp*IrCl)$_2$(rac-L^3)](BF$_4$)$_2$* ***(3b)*** *(Method A).* Yield: 11%. IR (KBr): ν 1471 (m), 1437 (m), 1084 (s), 1062 (s), 1031 (s) cm^{-1}. ESI-MS (MeOH): m/z 1255.30 (z1, [[(Cp*IrCl)$_2$(*rac*-L^3)](BF$_4$)]$^+$ (1255.27)). ^{1}H NMR (DMSO-d_6): δ 1.34 (s, 30H, Cp*), 1.78−3.21 (m, 6H, CH_2), 4.03−4.23 (m, 4H, $PyCH_2$), 6.40−8.56 (m, 18H, Ph, Py). ^{31}P{^{1}H} NMR (DMSO-d_6): δ 19.4 (s, 2P). Elemental analysis was not performed because only a small amount of the pure sample was isolated.

*[(Cp*RhCl)$_2$(meso-L^3)](BF$_4$)$_2$* ***(3c)*** *(Method A).* Yield: 12%. IR (KBr): ν 1472 (m), 1435 (m), 1084 (s), 1057 (s) cm^{-1}. ESI−MS (MeOH): m/z 1075.16 (z1, [[(Cp*RhCl)$_2$(*meso*-L^3)](BF$_4$)]$^+$ (1075.16)). ^{31}P{^{1}H} NMR (DMSO-d_6): δ 49.9 (d, 2P, J_{P-Rh} = 135 Hz). Elemental analysis was not performed because only small amount of the pure sample was isolated.

*[(Cp*RhCl)$_2$(rac-L^3)](BF$_4$)$_2$* ***(3d)*** *(Method A).* Yield: 4%. IR (KBr): ν 1472 (m), 1437 (m), 1084 (s), 1057 (s) cm^{-1}. ESI-MS (MeOH): m/z 1133.10 (z1, [[(Cp*RhCl)$_2$(*rac*-L^3)](PF$_6$)]$^+$ (1133.12)). ^{31}P{^{1}H} NMR (DMSO-d_6): δ 48.5 (d, 2P, J_{P-Rh} = 135 Hz). Elemental analysis was not performed because only a small amount of the pure sample was isolated. A similar procedure using NH_4PF_6 instead of NH_4BF_4 gave a small amount of the crystalline compound [(Cp*RhCl)$_2$(*rac*-L^3)](PF$_6$)$_2$·0.5Et$_2$O (**3d′**·0.5Et$_2$O), which was characterized by X-ray crystallography.

*[(Cp*IrCl)$_2$(meso-L^4)](BF$_4$)$_2$·0.5CH$_2$Cl$_2$* ***(4a·0.5CH$_2$Cl$_2$)*** *(Method A).* Yield: 4%. Anal. Calcd for $C_{48.5}H_{61}B_2Cl_3F_8Ir_2N_2P_2$: C, 41.66; H, 4.40; N, 2.00. Found: C, 41.86; H, 4.01; N, 2.07. IR (KBr): ν 1473 (m), 1436 (m), 1055 (s) cm^{-1}. ESI-MS (MeOH): m/z 591.17 (z2, [[(Cp*IrCl)$_2$(*meso*-L^4)]]$^{2+}$ (591.14)). ^{1}H NMR (CD_2Cl_2): δ 1.31 (m, 1H, CH_2), 1.42 (s, 30H, Cp*), 1.54 (m, 1H, CH_2), 1.66 (m, 1H, CH_2), 2.03−2.14 (m, 2H, CH_2), 2.34−2.43 (m, 2H, CH_2), 3.93 (dd, 2H, J = 17, 12 Hz, $PyCH_2$), 4.23 (dd, 2H, J = 17, 12 Hz, $PyCH_2$), 7.41−7.46 (m, 6H, Ph, Py), 7.57−7.59 (m, 6H, Ph), 7.99−8.01 (m, 4H, Py), 8.53 (d, 2H, J = 6 Hz, Py). ^{31}P{^{1}H} NMR (CD_2Cl_2): δ 19.5 (s, 2P).

*[(Cp*IrCl)$_2$(rac-L^4)](BF$_4$)$_2$·0.75CH$_2$Cl$_2$* ***(4b·0.75CH$_2$Cl$_2$)*** *(Method A).* Yield: 3%.

4b·0.75CH$_2$Cl$_2$ *(Method B).* To a solution of $[Cp^*IrCl_2]_2$ (50.4 mg, 0.063 mmol) in CH_2Cl_2 (5 mL) were added a solution of *rac*-L^4 (29.5 mg, 0.063 mmol) in CH_2Cl_2 (10 mL) and NH_4BF_4 (33.2 mg, 0.31 mmol), and the mixture was stirred overnight at room temperature

dx.doi.org/10.1021/om400965j | *Organometallics* 2013, 32, 7470−7477

before filtration. The filtrate was concentrated to ca. 3 mL. After addition of Et_2O (2 mL), the solution was allowed to stand in a refrigerator to afford yellow crystals of **4b**. Yield: 37 mg, 75%. Anal. Calcd for $C_{48.75}H_{61.5}B_2Cl_{3.5}F_8Ir_2N_2P_2$: C, 41.25; H, 4.37; N, 1.97. Found: C, 41.32; H, 4.23; N, 2.07. IR (KBr): ν 1470 (m), 1437 (m), 1055 (s) cm^{-1}. ESI-MS (MeOH): m/z 590.98 (z2, $[[(Cp^*IrCl)_2(meso\text{-}L^4)]]^{2+}$ (591.14)). ^1H NMR (CD_2Cl_2): δ 1.43 (d, 30H, J = 2 Hz, Cp*), 1.59 (m, 4H, CH_2), 2.00−2.13 (m, 2H, CH_2), 2.27−2.38 (m, 2H, CH_2), 3.93 (dd, 2H, J = 18, 11 Hz, $PyCH_2$), 4.20 (dd, 2H, J = 17, 12 Hz, $PyCH_2$), 7.39−7.47 (m, 6H, Ph, Py), 7.56−7.59 (m, 6H, Ph), 7.91 (d, 2H, J = 8 Hz, Py), 7.98 (t, 2H, J = 8 Hz, Py), 8.53 (d, 2H, J = 6 Hz, Py). $^{31}P\{^1H\}$ NMR (CD_2Cl_2): δ 18.5 (s, 2P).

*$[(Cp^*RhCl)_2(meso\text{-}L^4)](BF_4)_2$ (**4c**) (Method A).* Yield: 2%. IR (KBr): ν 1471 (m), 1437 (m), 1055 (s) cm^{-1}. ESI-MS (MeOH): m/z 1089.17 (z1, $[[(Cp^*RhCl)_2(meso\text{-}L^4)(BF_4)]]^+$ (1089.22)). $^{31}P\{^1H\}$ NMR (DMSO-d_6): δ 48.5 (d, 2P, J_{P-Rh} = 134 Hz). Elemental analysis was not performed because only a small amount of the pure sample was isolated.

*$[(Cp^*RhCl)_2(rac\text{-}L^4)](BF_4)_2\cdot 0.75CH_2Cl_2$ (**4d**$\cdot 0.75CH_2Cl_2$) (Method A).* Yield: 3%.

***4d**$\cdot 0.75CH_2Cl_2$ (Method B).* To a solution of $[Cp^*RhCl_2]_2$ (50.2 mg, 0.081 mmol) in CH_2Cl_2 (5 mL) were added a solution of *rac*-L^4 (37.1 mg, 0.081 mmol) in CH_2Cl_2 (10 mL) and NH_4BF_4 (42.2 mg, 0.40 mmol), and the mixture was stirred overnight at room temperature. The mixture was filtered and concentrated to ca. 3 mL, and after addition of Et_2O (2 mL), it was allowed to stand in a refrigerator to afford yellow crystals of **4b**. Yield: 74 mg, 77%. Anal. Calcd for $C_{48.75}H_{61.5}B_2Cl_{3.5}F_8N_2P_2Rh_2$: C, 47.18; H, 5.00; N, 2.26. Found: C, 47.14; H, 4.77; N, 2.31. IR (KBr): ν 1471 (m), 1436 (m), 1054 (s) cm^{-1}. ESI-MS (MeOH): m/z 1089.17 (z1, $[[(Cp^*RhCl)_2(meso\text{-}L^4)(BF_4)]]^+$ (1089.22)). ^1H NMR (CD_2Cl_2): δ 1.42 (d, 30H, J = 2 Hz, Cp*), 2.00−2.12 (m, 2H, CH_2), 2.32−2.44 (m, 2H, CH_2), 3.90 (dd, 2H, J = 16, 14 Hz, $PyCH_2$), 4.12 (dd, 2H, J = 17, 13 Hz, $PyCH_2$), 7.42−7.46 (m, 4H, Ph), 7.51 (t, 2H, J = 7 Hz, Py), 7.56−7.61 (m, 6H, Ph), 7.80 (d, 2H, J = 8 Hz, Py), 7.97 (t, 2H, J = 8 Hz, Py), 8.55 (d, 2H, J = 6 Hz, Py). $^{31}P\{^1H\}$ NMR (CD_2Cl_2): δ 47.9 (d, 2P, J_{P-Rh} = 132 Hz).

X-ray Crystallography. Crystals of *meso*-$L^2\cdot 2BH_3$, *rac*-$L^4\cdot 2BH_3$, **2a−c**, **3a**,**d**′, and **4a**,**b**,**d** were quickly coated with Paratone N oil and mounted on top of a loop fiber at room temperature. The crystal and experimental data are summarized in Tables S1−S3 (see the Supporting Information). All data were collected at −120 °C (**2a−c**, **3a**, **3d**′, **4a**) or −150 °C (*meso*-$L^2\cdot 2BH_3$, *rac*-$L^4\cdot 2BH_3$, **4b**,**d**) on a Rigaku AFC8/Mercury CCD diffractometer equipped with graphite-monochromated Mo Kα radiation using a rotating-anode X-ray generator (50 kV, 200 mA) and a Rigaku VariMax Mo/Saturn CCD diffractometer equipped with graphite-monochromated Mo Kα radiation using a rotating-anode X-ray generator (RA-Micro7, 50 kV, 24 mA). A total of 720−1440 oscillation images, covering a whole sphere of $6° < 2\theta < 55°$, were collected by the ω-scan method. The crystal-to-detector (70 × 70 mm) distance was set at 45 mm. The data were processed using the Crystal Clear 1.3.5 program (Rigaku/MSC)[8] and corrected for Lorentz−polarization and absorption effects.[9] The structures were solved by direct methods with SHELXS-97[10] (**2a**,**b**, **4b**) and SIR-92[11] (*meso*-$L^2\cdot 2BH_3$, *rac*-$L^4\cdot 2BH_3$, **2c**, **3a**, **3d**′, **4a**,**d**) and were refined on F^2 with full-matrix least-squares techniques with SHELXL-97[10] using the Crystal Structure 4.0 package.[12] All non-hydrogen atoms were refined with anisotropic thermal parameters, and the C−H hydrogen atoms were calculated at ideal positions and refined with riding models. All calculations were carried out on a Windows PC running the Crystal Structure 4.0 package.[12]

■ ASSOCIATED CONTENT

Supporting Information

Tables of crystallographic data for *meso*-$L^2\cdot 2BH_3$, *rac*-$L^4\cdot 2BH_3$, **2a−c**, **3a**, **3d**′, and **4a**,**b**,**d**, CIF files giving the structural parameters for **2a−c**, **3a**, **3d**′, and **4a**,**b**,**d**, ORTEP diagrams of *meso*-$L^2\cdot 2BH_3$, *rac*-$L^4\cdot 2BH_3$, **2c**, and **4d**, plots of metal−metal separations of **2a−c**, **3a**, **3d**′, and **4a**,**b**,**d**, and van't Hoff plots for **2a**,**b**, **3a**,**b**, and **4a**,**d**. This material is available free of charge via the Internet at http://pubs.acs.org.

■ AUTHOR INFORMATION

Corresponding Authors

*T.N.: e-mail, t.nakajima@cc.nara-wu.ac.jp; fax, +81 742-20-3847; tel, +81 742-20-3847.

*T.T.: e-mail, tanase@cc.nara-wu.ac.jp.

Notes

The authors declare no competing financial interest.

■ ACKNOWLEDGMENTS

This work was supported by a Grant-in-Aid for Scientific Research and on Priority Area 2107 (Nos. 22108521, 24108727) from the Ministry of Education, Culture, Sports, Science and Technology of Japan. T.N. is grateful to Tokuyama Science Foundation, Kurata Memorial Hitachi Science and Technology Foundation, and Nara Women's University for a research project grant.

■ REFERENCES

(1) (a) Puddephatt, R. J. *Chem. Soc. Rev.* **1983**, *12*, 99−127. (b) Broussard, M. E.; Juma, B.; Train, S. G.; Peng, W.-J.; Laneman, S. A.; Stanley, G. G. *Science* **1993**, *260*, 1784−1788. (c) Bader, A.; Linder, E. *Coord. Chem. Rev.* **1991**, *108*, 27−110. (d) Bessel, C. A.; Aggarwal, P.; Marschilok, A. C.; Takeuchi, K. J. *Chem. Rev.* **2001**, *101*, 1031−1066.

(2) For recent examples, see: (a) Angamuthu, R.; Byers, P.; Lutz, M.; Spek, A. L.; Bouwman, E. *Science* **2010**, *327*, 313−315. (b) Matano, Y.; Miyajima, T.; Nakabuchi, T.; Imahori, H.; Ochi, N.; Sakaki, S. *J. Am. Chem. Soc.* **2006**, *128*, 11760−11761. (c) Gagliardo, M.; Selander, N.; Mehendale, N. C.; van Koten, G.; Gebbink, R. J. M. K.; Szabó, K. J. *Chem. Eur. J.* **2008**, *14*, 4800. (d) Lee, C.-C.; Ke, W.-C.; Chan, K.-T.; Lai, C.-L.; Hu, C.-H.; Lee, H. M. *Chem. Eur. J.* **2007**, *15*, 582−591. (e) Miranda-Soto, V.; Grotjahn, D. B.; Dipasquale, A. G.; Rheingold, A. L. *J. Am. Chem. Soc.* **2008**, *130*, 13200−13201.

(3) For our recent examples, see: (a) Nakajima, T.; Sakamoto, M.; Kurai, S.; Kure, B.; Tanase, T. *Chem. Commun.* **2013**, *49*, 5239−5338. (b) Kure, B.; Nakajima, T.; Tanase, T. *J. Organomet. Chem.* **2013**, *733*, 28−35. (c) Goto, E.; Begum, R.; Hosokawa, A.; Yamamoto, C.; Kure, B.; Nakajima, T.; Tanase, T. *Organometallics* **2012**, *31*, 8482−8497. (d) Kure, B.; Taniguchi, A.; Nakajima, T.; Tanase, T. *Organometallics* **2012**, *31*, 4791−4800. (e) Nakajima, T.; Kurai, S.; Noda, S.; Zouda, M.; Kure, B.; Tanase, T. *Organometallics* **2012**, *31*, 4283−4294 and references cited therein. (f) Yoshii, A.; Takenaka, H.; Nagata, H.; Noda, S.; Nakamae, K.; Kure, B.; Nakajima, T.; Tanase, T. *Organometallics* **2012**, *31*, 133−143. (g) Takemura, Y.; Nakajima, T.; Tanase, T. *Eur. J. Inorg. Chem.* **2009**, 4820−4829. (h) Takemura, Y.; Takenaka, H.; Nakajima, T.; Tanase, T. *Angew. Chem., Int. Ed.* **2009**, *48*, 2157−2161.

(4) (a) Fache, F.; Schulz, E.; Tommasino, M. L.; Lemaire, M. *Chem. Rev.* **2000**, *100*, 2159−2231. (b) Newkome, G. R. *Chem. Rev.* **1993**, *93*, 2067−2089. (c) Espinet, P.; Soulantica, K. *Coord. Chem. Rev.* **1999**, *193−195*, 499−556. (d) Braunstein, P.; Naud, F. *Angew. Chem., Int. Ed.* **2001**, *40*, 680−699. (e) Speiser, F.; Braunstein, P.; Saussine, L. *Acc. Chem. Res.* **2005**, *38*, 784−793. (f) Flapper, J.; Kooijman, H.; Lutz, M.; Spek, A. L.; van Leeuwen, P. W. N. M.; Elsevier, C. J.; Kamer, P. C. J. *Organometallics* **2009**, *28*, 1180−1192. (g) Dubs, C.; Yamamoto, T.; Inagaki, A.; Akita, M. *Chem. Commun.* **2006**, 1962−1964. (h) Li, P.; Wang, M.; Chen, L.; Liu, J.; Zhao, Z.; Sun, L. *Dalton Trans.* **2009**, 1919−1926. (i) Aguirre, P. A.; Lagos, C. A.; Moya, S. A.; Zúñiga, C.; V.-Oyarce, C.; Sola, E.; Peris, G.; Bayón, J. C. *Dalton Trans.* **2007**, 5419−5426. (j) Speiser, F.; Braunstein, P.; Saussine, L. *Organometallics* **2004**, *23*, 2625−2632. (k) de la Encarnación, E.; Pons, J.; Yáñez, R.; Ros, J. *Inorg. Chim. Acta* **2006**, *359*, 745−752. (l) Hung-Low, F.;

Klausmeyer, K. K. *Inorg. Chim. Acta* **2008**, *361*, 1298−1310. (m) Chen, H.-P.; Liu, Y.-H.; Peng, S.-M.; Liu, S.-T. *Organometallics* **2003**, *22*, 4893−4899. (n) Flapper, J.; Kooijman, H.; Lutz, M.; Spek, A. L.; van Leeuwen, P. W. N. M.; Elsevier, C. J.; Kamer, P. C. J. *Organometallics* **2009**, *28*, 3272−3281. (o) Braunstein, P.; Heaton, B. T.; Jacob, C.; Manzi, L.; Morise, X. *Dalton Trans.* **2003**, 1396−1401. (p) Yang, H.; Lugan, N.; Mathieu, R. *Organometallics* **1997**, *16*, 2089−2095. (q) Mothes, E.; Sentes, S.; Luquin, M. A.; Mathieu, R.; Lugan, N.; Lavigne, G. *Organometallics* **2008**, *27*, 1193−1206. (r) Brunner, H.; Valério, C.; Zabel, M. *New J. Chem.* **2000**, *24*, 275−279. (s) Chen, H.-P.; Liu, Y.-H.; Peng, S.-M.; Liu, S.-T. *Dalton Trans.* **2003**, 1419−1424. (t) Aguirre, P. A.; Lagos, C. A.; Moya, S. A.; Zúñiga, C.; V.-Oyarce, C.; Sola, E.; Peris, G.; Bayón, J. C. *Dalton Trans.* **2007**, 5419−5426. (u) Green, M. J.; Cavell, K. J.; Edwards, P. G.; Tooze, R. P.; Skelton, B. W.; White, A. H. *Dalton Trans.* **2004**, 3251−3260. (v) Liu, Z.; Djurovich, P. I.; Whited, M. T.; Thompson, M. E. *Inorg. Chem.* **2012**, *51*, 230−236. (w) Jiménze-Tenorio, M.; Puerta, M. C.; Valerga, P.; Moncho, S.; Ujaque, G.; Lledós, A. *Inorg. Chem.* **2010**, *49*, 6035−6057. (x) Liu, F.; Pullarkat, S. A.; Li, Y.; Chen, S.; Yuan, M.; Lee, Z. Y.; Leung, P.-H. *Organometallics* **2009**, *28*, 3941−3946.

(5) (a) Catalano, V. J.; Kar, H. M.; Garnas, J. *Angew. Chem. Int. Ed.* **1999**, *38*, 1979−1982. (b) Catalano, V. J.; Bennett, B. L.; Yson, R. L.; Noll, B. C. *J. Am. Chem. Soc.* **2000**, *122*, 10056−10062. (c) Catalano, V. J.; Bennett, B. L.; Kar, H. M. *J. Am. Chem. Soc.* **1999**, *121*, 10235−10236. (d) Catalano, V. J.; Malwitz. *J. Am. Chem. Soc.* **2004**, *126*, 6560−6561. (e) Catalano, V. J.; Malwitz, J.; Noll, B. C. *Inorg. Chem.* **2002**, *41*, 6553−6559. (f) Catalano, V. J.; Bennett, B. L.; Noll, B. C. *Chem. Commun.* **2000**, 1413−1414. (g) Uang, R.-H.; Chan, C.-K.; Peng, S.-M.; Che, C.-M. *Chem. Commun.* **1994**, 2561−2562. (h) Tanase, T.; Igoshi, T.; Kobayashi, Y.; Yamamoto, Y. *J. Chem. Res.(S)* **1998**, 538. (i) Catalano, V. J.; Kar, H. M.; Bennett, B. L. *Inorg. Chem.* **2000**, *39*, 121−127. (j) Goto, E.; Usuki, M.; Takenaka, H.; Sakai, K.; Tanase, T. *Organometallics* **2004**, *23*, 6042. (k) Tanase, T.; Takenaka, H.; Goto, E. *J. Organomet. Chem.* **2007**, *692*, 175−183. (l) Schenck, T. G.; Milne, C. R. C.; Sawyer, J. F.; Bosnich, B. *Inorg. Chem.* **1985**, *24*, 2338. (m) Tanaka, S.; Akita, M. *Angew. Chem., Int. Ed.* **2001**, *40*, 2865−2867. (n) Tanaka, S.; Dubs, C.; Inagaki, A.; Akita, M. *Organometallics* **2004**, *23*, 317−319. (o) Tanaka, S.; Dubs, C.; Inagaki, A.; Akita, M. *Organometallics* **2004**, *24*, 163−184. (p) Yamaguchi, T.; Koike, T.; Akita, M. *Organometallics* **2010**, *29*, 6493−6502.

(6) (a) Hounjet, L. J.; Bierenstiel, M.; Ferguson, M.; McDonald, R.; Cowie, M. *Dalton Trans.* **2009**, 4213−4226. (b) Bennett, J.; Rae, A. D.; Salem, G.; Ward, N. C.; Warling, P.; Wells, K.; Willis, A. C. *Dalton Trans.* **2002**, 234−243. (c) Gómez, M.; Jansat, S.; Muller, G.; Panyella, D.; van Leeuwen, P. W. N. M.; Kamer, P. C. J.; Goubitz, K.; Fraanje, J. *Organometallics* **1999**, *18*, 4970−4981. (d) Jones, N. D.; Meessen, P.; Smith, M. B.; Losehand, U.; Retting, S. J.; Patrick, B. O.; James, B. R. *Can. J. Chem.* **2002**, *80*, 1600−1606. (e) Budzelaar, P. H. M.; Frijns, J. H. G. *Organometallics* **1990**, *9*, 1222−1227. (f) Jones, N. D.; Meessen, P.; Losehand, U.; Patrick, B. O.; James, B. R. *Inorg. Chem.* **2005**, *44*, 3290. (g) Cagnolini, A.; Ballard, B.; Engelbrecht, H. P.; Rpld, T. L.; Barnes, C.; Cutler, C.; Hoffman, T. J.; Kannan, R.; Katti, K.; Jurisson, S. S. *Nucl. Med. Biol.* **2011**, *38*, 63−76. (h) Ansell, C. W. G.; Cooper, M. K.; Dancey, K. P.; Duckworth, P. A.; Henrick, K.; McPartlin, M.; Organ, G.; Tasker, P. A. *J. Chem. Soc., Chem. Commun.* **1985**, 437−439. (i) Müller, G.; Klinga, M.; Leskelä; Rieger, B. *Eur. J. Inorg. Chem.* **2002**, 2625−2632.

(7) (a) Brunner, H.; Köllnberger, A.; Mehmood, A.; Tsuno, T.; Zabel, M. *J. Organomet. Chem.* **2004**, *689*, 4244−4262. (b) Brunner, H.; Ike, H.; Muschiol, M.; Tsuno, T.; Koyama, K.; Kurosawa, T.; Zabel, M. *Organometallics* **2011**, *30*, 3666−3676. (c) Brunner, H.; Muschiol, M.; Tsuno, T.; Ike, H.; Kurosawa, T.; Koyama, K. *Angew. Chem., Int. Ed.* **2012**, *51*, 1067−1070. (d) Brunner, H.; Tsuno, T. *Acc. Chem. Res.* **2009**, *42*, 1501−1510.

(8) Gómes, M.; Jansat, S.; Muller, G.; Panyella, D.; van Leeuwen, P. W. N. M.; Kamer, P. C. J.; Goubitz, K.; Fraanje, J. *Organometallics* **1999**, *18*, 4970−4981.

(9) *Crystal Clear, version 1.3.5, Operating software for the CCD detector system*, Rigaku and Molecular Structure Corp., Tokyo, Japan, and The Woodlands, TX, USA, 2003.

(10) Jacobson, R. *REQAB*; Molecular Structure Corp., The Woodlands, TX, USA, 1998.

(11) Sheldrick, G. M. *SHELXL-97: Program for the Refinement of Crystal Structures*; University of Göttingen, Göttingen, Germany, 1996.

(12) (a) Altomare, A.; Burla, M. C.; Camalli, M.; Cascarano, M.; Giacovazzo, C.; Guagliardi, A.; Polidori, G. *J. Appl. Crystallogr.* **1994**, *27*, 435−436. (b) Altomare, A.; Burla, M.; Camalli, M.; Cascarano, G.; Giacovazzo, C.; Guagliardi, A.; Moliterni, A.; Polidori, G.; Spagna, R. *J. Appl. Crystallogr.* **1999**, *32*, 115−119.

(13) *CrystalStructure 4.0: Crystal Structure Analysis Package*, Rigaku Corp., Tokyo 196-8666, Japan, 2000−2010.